J. Physiol. (1976), **255**, *pp.* 157–189
With 15 text-figures
Printed in Great Britain

THE TEMPORAL AND STEADY-STATE RELATIONSHIPS BETWEEN ACTIVATION OF THE SODIUM CONDUCTANCE AND MOVEMENT OF THE GATING PARTICLES IN THE SQUID GIANT AXON

BY R. D. KEYNES AND E. ROJAS*

From the Laboratory of the Marine Biological Association, Plymouth, and the Physiological Laboratory, Cambridge CB2 3EG

(*Received 9 June 1975*)

SUMMARY

1. Comparisons were made between the kinetics and steady-state properties of the sodium conductance changes and of the sodium gating currents, in the squid giant axon perfused with caesium fluoride and maintained at a high membrane holding potential. The conductance measurements were made with reduced external sodium and as much electrical compensation as possible, in order to minimize errors caused by the series resistance.

2. After an initial delay of 10–150 μsec whose size was a function of the holding potential and pulse amplitude, the conductance rise on depolarization followed cube law kinetics.

3. Values of the time constant τ_m, as defined by Hodgkin & Huxley (1952*b*), were determined for membrane potentials ranging between -140 and $+70$ mV. They lay on a nearly symmetrical bell-shaped curve with a maximum (at 6·3° C) of just under 500 μsec at -36 mV.

4. Values of the gating current time constant τ(V) were determined over the same potential range, and found to lie on a very similar bell-shaped curve. A computed least-squares best fit gave the maximum as 460 μsec, also falling at about -36 mV.

5. The midpoint of the m_∞ curve lay at -34 mV, and its slope at this point was 0·0139 mV^{-1}. Another series of measurements on intact axons gave a midpotential of -25 mV. In the perfused axons the state of the membrane was better described by the constant field equation than by g_{Na}. Recalculation of m_∞ from P_{Na} shifted the curve about 15 mV in a positive direction.

* Present address: Biophysics, School of Biological Sciences, University of East Anglia, Norwich NOR 88C.

6. The midpoint of the normalized steady-state gating charge distribution curve lay at -26 mV, where its slope was 0·0135 mV^{-1}.

7. The ratio of the limiting slopes of the curves for sodium conductance and for gating charge distribution plotted against potential was close to 3:1, confirming the previous conclusion that each sodium channel behaves as if it incorporated three gating particles.

8. At a high holding potential, the time constant for shutting off the sodium conductance at the end of a large pulse was shown to be close to one third of the gating current time constant, as predicted by cube law kinetics. An explanation is provided for the failure of this relationship to hold good for small depolarizing pulses.

9. The rather close quantitative agreement between the behaviour of the sodium conductance system and the properties of the mobile charges whose movements generate the asymmetrical displacement current, provides persuasive support for the identification of these charges as the sodium gating particles.

INTRODUCTION

Both in the squid giant axon (Armstrong & Bezanilla, 1974; Keynes & Rojas, 1974; Meves, 1974) and at the node of Ranvier in frog nerve (Nonner, Rojas & Stämpfli, 1975) the capacity currents that flow across the membrane on application of equal positive and negative voltage-clamp steps are asymmetrical. It seems clear that the asymmetry arises from the presence of mobile charged particles forming an integral part of the membrane, because for brief pulses at least the total transfer of charge (1) is equal and opposite at the beginning and end of the pulse, (2) reaches saturation when the internal potential is taken to a sufficiently positive value, and (3) is the same size at all temperatures, although its time constant has a large temperature coefficient. Our initial analyses (Keynes & Rojas, 1974; Rojas & Keynes, 1975) indicated that these mobile charges possessed many of the attributes of the hypothetical gating particles that control the opening of the sodium channels on depolarization of the membrane (Hodgkin & Huxley, 1952*b*). Thus (1) their relaxation time constants agreed fairly well both in absolute magnitude and in voltage dependence with the values obtained by Hodgkin & Huxley (1952*b*) for τ_m; (2) the potential at which the particles were evenly distributed between their two energy states was reasonably close to the midpoint of the m_∞ curve; (3) the evidence suggested that there were three particles per channel, in accordance with m^3 kinetics; (4) the total amount of mobile charge fitted approximately with estimates of the number of high affinity tetrodotoxin binding sites (Keynes, Bezanilla, Rojas & Taylor, 1975; Levinson & Meves, 1975). However, there were some difficulties in making

this identification, especially concerning the precise relationship between the time constants for closing the sodium channels and for restoration of the mobile charges to their original position at the end of a pulse. In this paper we present a critical comparison between the kinetics of the mobile charges and of the sodium conductance, and between the steady-state properties of the two systems, from measurements made as far as possible on the same axons with careful attention to errors arising from sources such as imperfect compensation for the electrical resistance in series with the membrane. In order to avoid the complications that arise during maintained depolarization of the membrane (Meves, 1974; Keynes, Rojas & Rudy, 1974; Keynes, 1975), we only consider here experiments conducted with holding potentials between -60 and -140 mV.

METHODS

The experiments were performed with giant axons 500–900 μm in diameter dissected from the hindmost stellar nerve in mantles from *Loligo forbesi* or occasionally *L. vulgaris*. The majority of the experiments in which gating currents were measured were performed with axons perfused intracellularly (Rojas, Taylor, Atwater & Bezanilla, 1969). For some of the measurements of sodium conductance, the fibres were mounted intact in the same chamber, with an axial 100 μm platinum wire coated with platinum black inserted longitudinally through a cut at one end to carry the applied current, and a 100 μm micropipette filled with 500 mM potassium chloride inserted at the other end to record the internal potential. The gating currents were measured as described by Keynes & Rojas (1974).

Solutions

The composition of the solutions used is given in Table 1. All were prepared with double-glass-distilled water. Solutions containing tetrodotoxin were prepared by adding the toxin from a 30 μM stock solution in distilled water. The pH of all solutions was adjusted to $7{\cdot}3 \pm 0{\cdot}2$ at 10° C.

The conductivity of each solution listed in Table 1 was compared at 20° C with that of artificial sea water made with chloride, using platinum electrodes in a standard glass cell (Radiometer Conductivity Meter, Model CDM 2).

The chemical activity of sodium, potassium, chloride and calcium ions was measured in each solution at 15° C, and compared with that of the same ion in chloride sea water. Sodium, potassium and chloride activities were measured with solid-state electrodes, and calcium activity was measured with an ion exchange membrane electrode, using an Orion Digital pH/mV Meter, Model 801.

Experimental procedure

Normally the axons were first bathed in potassium-free sea water (Na–SW of Table 1) for a few min, and were then internally perfused with either potassium fluoride or caesium fluoride. A few experiments were performed with intact unperfused axons. Next the external solution was replaced by one containing quarter of the usual amount of sodium ($\frac{1}{4}$Na–SW). A standard voltage-clamp run was then carried out, using an amplifier system with positive feed-back to compensate as far as possible for the effect of the resistance R_s in series with the axon membrane, up

TABLE 1. Ionic composition and some properties of the solutions used

	Na^+ (mM)	$Tris^+$ (mM)	Ca^{2+} (mM)	Mg^{2+} (mM)	Relative ionic activity at 15° C. Cl^-	Na^+	Ca^{2+}	Relative conductivity	Osmotic pressure (m-osmole)
A. External chloride solutions									
Na–SW	430	5	10	50	1·000	1·000	1·000	1·00	1020
Tris–SW	—	435	10	50	0·689	0·001	0·890	0·60	970
¾Na–SW	322·5	107·5	10	50	0·970	0·730	0·870	0·95	1006
½Na–SW	215	220	10	50	0·930	0·460	0·840	0·86	994
¼Na–SW	107·5	322·5	10	50	0·758	0·265	0·870	0·68	1002
B. External isethionate solutions									
Na–SW-1	430	5	10	50	0·205	0·797	0·840	0·678	1240
Na–SW-2	430	5	15	50	0·010	0·800	1·050	0·682	1241
Tris–SW-1	—	435	10	50	0·198	0·005	0·800	0·420	997
Tris–SW-2	—	435	15	50	0·008	0·006	0·950	0·420	1010
C. External acetate solutions									
Na–SW	430	5	10	50	0·207	0·743	1·100	0·599	960
Tris–SW	—	435	10	50	0·180	0·001	0·980	0·385	1080

D. Internal fluoride solutions

	K^+ (mM)	Cs^+ (mM)	Tris Cl (mM)	Sucrose (mM)	Relative conductivity	Osmotic pressure (-osmole)
High K^+	550	—	10	—	0·960	970
High Cs^+-1	—	300	10	400	0·486	1300
High Cs^+-2	—	350	10	400	0·510	1350
Low Cs^+	—	50	10	900	0·067	1370

to a maximum of 5 Ω cm². When the characteristics of the sodium conductance system had been determined, the external solution was replaced by a sodium-free saline (Tris–SW) with 300 nM tetrodotoxin, and 10–30 min later the axon was ready for observation of the gating currents. On completion of the displacement current runs, ¼Na–SW was re-introduced into the chamber, and 30–60 min were allowed for recovery before making the final set of voltage-clamp records. In the majority of the experiments the sodium currents were fully restored.

Measurements of series resistance

R_s was measured by the methods described by Moore & Cole (1962) and Keynes, Rojas, Taylor & Vergara (1973). Fig. 1 shows records of the initial change in membrane potential in intact (*B*) and perfused (*A*) axons under current-clamp conditions, and Table 2 summarizes the quantities calculated from such records. The total membrane capacity was obtained from

$$C_m = \frac{\Delta I}{dV/dt}, \tag{1}$$

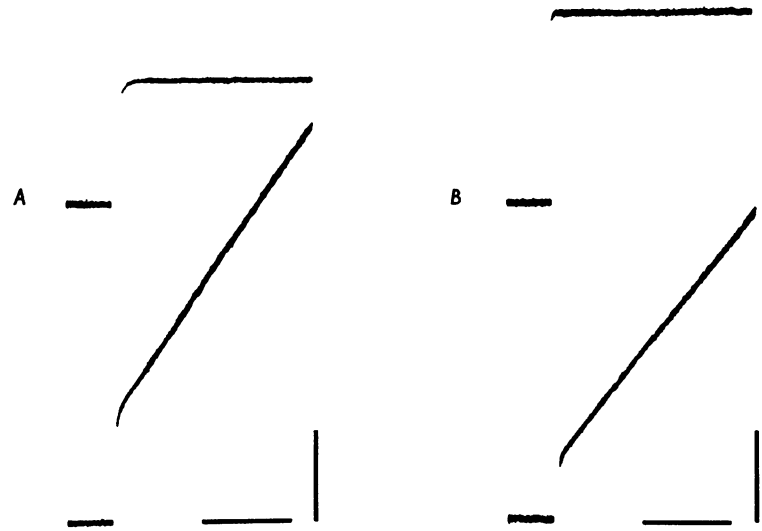

Fig. 1. Membrane potential transients recorded under current clamp conditions. The upper traces are membrane currents; the lower traces are the membrane potential transients. *A*, experiment 1-D-1, perfused fibre. Displacement of membrane current equal to 27 μA; dV/dt = 716 V/sec; C_m = 0·038 μF; R_s = 11·5 Ω cm². *B*, experiment 30-N-1 (1971), intact fibre. Displacement of membrane current equal to 41·5 μA; dV/dt = 610 V/sec; C_m = 0·068 μF; R_s = 4·4 Ω cm². Calibrations: vertical bar = 1 cm of the oscilloscope screen; horizontal bar = 10 μsec.

where ΔI represents the size of the current pulse, and dV/dt the slope of the potential record. The total series resistance was obtained from $\Delta V/\Delta I$, where ΔV was the size of the initial jump in the voltage transient. In order to arrive at values for the specific resistance in Ωcm², the membrane area was calculated both from πdL, where d was the fibre diameter and the length L of the external current electrodes was

0·25 cm, and from C_m, taking the specific capacity as 1 μF/cm^2 (Hodgkin & Huxley, 1952*b*). Agreement between the two estimates was generally rather good, and their over-all averages were exactly the same. The resistance was made up of two components, R_{ext} mostly being generated in the narrow gaps between neighbouring Schwann cells (Frankenhaeuser & Hodgkin, 1956), while R_{int} arose in the layer of axoplasm and perfusion solution between the internal current electrode and the membrane. As may be seen from the Table, the axons perfused with high ionic strength solutions had only a slightly higher R_s than intact axons, but perfusion with low ionic strength greatly increased the contribution of R_{int}. R_{ext} was raised by 1–3 Ωcm^2 on substituting tris for sodium in the external medium, and further still when isethionate replaced chloride, though no reliable measurements were made under these conditions.

TABLE 2. Membrane parameters determined under current-clamp conditions

(*a*) Condition of axon	(*b*) Measured membrane area $\pi d.L$ (cm^2)	(*c*) Measured membrane capacity $\Delta I/(\mathrm{d}V/\mathrm{d}t)$ (μF)	(*d*) Total resistance in series, $R_{ext}+R_{int}$ (Ω)	(*e*) Measured specific capacity (*c*)/(*b*) (μF/cm^2)	(*f*) Calculated specific series resistance $\frac{1}{2}[(b)+(c)]\times(d)$ (Ω cm^2)
Intact, in Na–SW	0·056	0·072	72·5	1·29	(13) 4·6 ± 0·4
Perfused high K$^+$, in Na–SW	0·071	0·068	82·0	0·96	(25) 5·7 ± 0·5
Perfused high K$^+$, in Tris–SW	0·073	0·069	123·9	0·95	(4) 8·8 ± 0·5
Perfused high Cs$^+$, in Na–SW	0·052	0·051	186·0	0·98	(3) 9·6 ± 0·4
Perfused high Cs$^+$, in Tris–SW	0·052	0·048	212·0	0·92	(5) 10·6 ± 0·9
Perfused low Cs$^+$, in Na–SW	0·065	0·063	423·4	0·97	(2) 27·1
Perfused low Cs$^+$, in Tris–SW	0·071	0·065	417·2	0·92	(2) 28·4

d = diameter; L = length of the external current electrodes = 0·25 cm. ( ): number of fibres. For column (*f*), the measured membrane area was averaged with the figure given by column (*c*), taking the true specific capacity of the membrane as 1 μF/cm^2.

The average peak inward sodium current measured during the recovery run in fibres perfused with a low caesium solution and bathed in sodium sea-water was 2·15 mA/cm^2 (Keynes & Rojas, 1974, Table 2). With no compensation for R_s, the voltage error would have been 27·1 × 2·15 = 58·3 mV, and even with the maximum compensation compatible with stability of the voltage-clamp system it would have been nearly 50 mV. Under these conditions, the time constants for switching the sodium conductance on and off would be hopelessly distorted. Reduction of the external sodium to $\frac{1}{4}$ lowered the peak current to 0·6 mA/cm^2, which with an axon perfused with high caesium and maximum R_s compensation gave a voltage error of only 3 mV.

Capacity transients

Fig. 2*A* shows the current transients recorded under voltage-clamp conditions in a fibre perfused with low caesium ion content and bathed in Tris–SW, and Fig. 2*B* is a similar record with high caesium perfusion. The membrane potential (referred always to the external solution as ground) was in each case displaced by 100 mV in a depolarizing direction, giving rise to an outward current transient. The inward transients for 100 mV hyperpolarizing pulses were close to mirror images of these records.

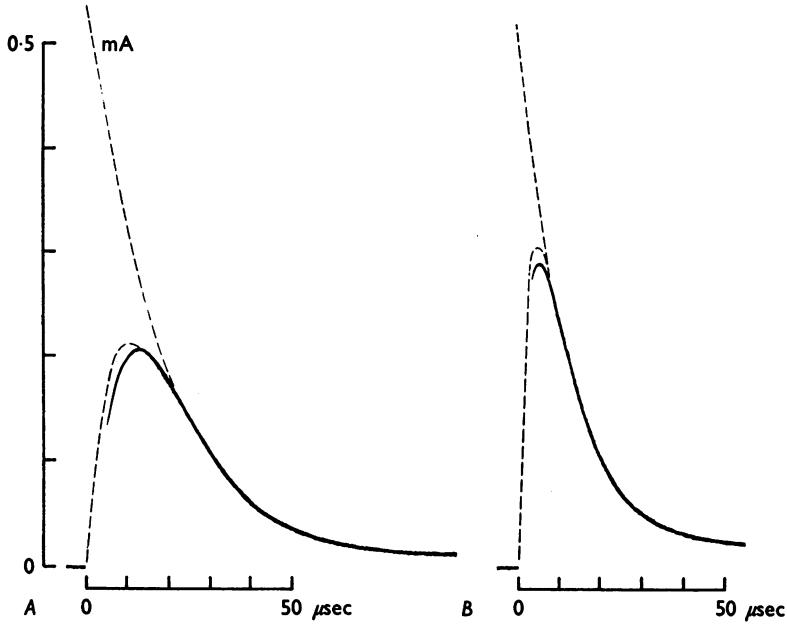

Fig. 2. Fast symmetrical current transients under voltage clamp. *A*, expt. 20–N–3, fibre perfused with low caesium in Tris–SW at 5·5° C. $V_h = -100$ mV; $V_p = 0$ mV. Dashed curves were calculated from eqn. (1) with $a = 0{\cdot}54$ mA, $b = 0{\cdot}054$ μsec^{-1}, $c = 0{\cdot}167$ μsec^{-1}. *B*, expt. 13–D–1, fibre perfused with high caesium in Tris–SW at 7·8° C. $V_h = -80$ mV; $V_p = 20$ mV. Dashed curves were calculated with $a = 0{\cdot}52$ mA, $b = 0{\cdot}087$ μsec^{-1}, $c = 0{\cdot}500$ μsec^{-1}.

The finite charging and discharging time of the membrane capacity arose because the membrane potential step was distorted by incomplete compensation for R_s. As a first approximation, the time course of the transients could be represented as

$$I = a(e^{-bt} - e^{-ct}). \tag{2}$$

For Fig. 2*A*, $a = 0{\cdot}54$ mA, $b = 0{\cdot}054$ μsec^{-1}, $c = 0{\cdot}167$ μsec^{-1}. The charge entering the capacity is

$$Q = \int_0^\infty I.\mathrm{d}t = C_m \times \text{pulse size}.$$

Since Q worked out as 6·35 nC, and the pulse was 100 mV, C_m was 0·0635 μF, in good agreement with an estimate of 0·06 μF from the current clamp data for this axon, and a membrane area of 0·067 cm^2.

From the value of b for Fig. 2B, the resistance in series with the capacitative element was calculated as 11·5 Ω cm^2, and the average for three experiments was 11·1 Ω cm^2. The current-clamp measurements gave 10·6 Ω cm^2.

Taking the total resistance R_s for fibres bathed in sodium sea-water and perfused with high potassium as 5·7 Ω cm^2 (Table 2), and for fibres bathed in Tris–SW and perfused with high caesium as 10·6 Ω cm^2, the conductivity data of Table 1 gives

$$5{\cdot}7 = R_{ext} + R_{int},$$
$$10{\cdot}6 = 1{\cdot}66R_{ext} + 1{\cdot}97R_{int}.$$

This system is satisfied for R_{ext} = 2·03 Ω cm^2 and R_{int} = 3·67 Ω cm^2.

Junction potentials

Junction potentials defined as the static potential difference between two solutions electrically connected together through a 3 M potassium chloride-agar bridge were measured with the electrode arrangement also used to measure the membrane potential. The following were typical values:

Na–SW//Tris–SW = −10 mV (negative the Na–SW),
Na–SW//high potassium = +5 mV,
Na–SW//high caesium = −15 mV,
Tris–SW//high potassium = +15 mV,
Tris–SW//high caesium = +12 mV, and
Tris–SW//low caesium = +3 mV.

All the solutions used for these measurements were prepared using chloride salts.

RESULTS

Kinetic properties of the sodium system

The main object of these experiments was to make an accurate comparison between the kinetic and steady-state properties of the sodium conductance on the one hand and the gating currents on the other. Since the gating current measurements covered a much wider range of membrane potentials than the conductance measurements of Hodgkin & Huxley (1952b) and others, it was first necessary to measure the rate at which the sodium current was turned on and off at a series of potentials from −140 to +70 mV. For this purpose, positive feed-back was applied to compensate as far as possible for the series resistance, and the external sodium was lowered to a quarter of the amount in normal sea water so as to reduce I_{Na} and minimize residual errors in the time constant of g_{Na} arising from incomplete compensation. Tris–Cl was substituted for sodium chloride in the $\frac{1}{4}$Na–SW (Table 1) in order to maintain tonicity and ionic strength. The time course of the initial rise in I_{Na} was then recorded for a series of potential steps from holding potentials ranging from −50 to −140 mV, and the rate at which I_{Na} was turned off on repolarization was measured at different times. Some typical traces are

illustrated in Fig. 3, from which it is seen that the time constant of the sodium current tail was independent of the pulse duration, but was decreased from 101 to 36 μsec on raising the holding potential from -60 to -100 mV. As shown in Table 4, this time constant was also independent of pulse size.

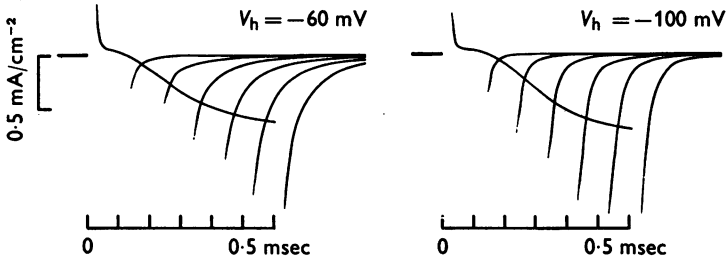

Fig. 3. I_{Na} transients during turn-off of g_{Na}. Expt. 20–D–1: fibre perfused with high caesium in $\frac{1}{4}$Na–SW at 7° C. R_s compensation set for 5 Ωcm^2. $V_p = 20$ mV for both records. For the record obtained with $V_h = -60$ mV, the curve fitting procedure gave $\delta t = 0$, τ_m for rise of $g_{Na} = 202$ μsec. The time constant for the I_{Na} tails during g_{Na} turn-off was 101 μsec ($\tau_m = 303$ μsec). For $V_h = -100$ mV, $\delta t = 30$ μsec and $\tau_m = 210$ μsec. The I_{Na} tail time constant was 36 μsec ($\tau_m = 108$ μsec).

In order to calculate values for τ_m as defined by Hodgkin & Huxley (1952*b*) we proceeded as follows:

(i) For each depolarizing voltage-clamp pulse in $\frac{1}{4}$Na–SW we obtained a membrane current trace which was digitalized at 25 μsec intervals. From the corresponding record in Tris–SW plus 300 nM tetrodotoxin we obtained its capacitative, gating and leakage components.

(ii) The inactivation time constant τ_h was determined by fitting an exponential to the values of I_{Na} obtained after m could safely be assumed to have reached m_∞, that is to say over the last 10 msec of the 15 msec pulses used when the potential during the pulse, V_p, did not go beyond 0 mV, or over the last 5 msec of the 8 msec pulses used when V_p was taken to a positive value.

(iii) I_{Na} was next divided by exp $(-t/\tau_h)$ in order to obtain instantaneous current values I'_{Na}, together with estimates of the peak current I^∞_{Na} for each pulse, each corrected for inactivation.

(iv) τ_m was determined from the slope of a semilogarithmic plot of $(1 - \sqrt[3]{(I'_{Na}/I^\infty_{Na})}$ against time. In accordance with m^3 kinetics (see eqn. (19) of Hodgkin & Huxley, 1952*b*), these plots gave excellent straight lines, but except at the lowest holding potentials they did not pass through $t = 0$, indicating that there was finite delay δt before I_{Na} began to rise.

(v) For a number of the runs, the values of I'_{Na} were submitted to a least-squares curve fitting procedure with a computer program which

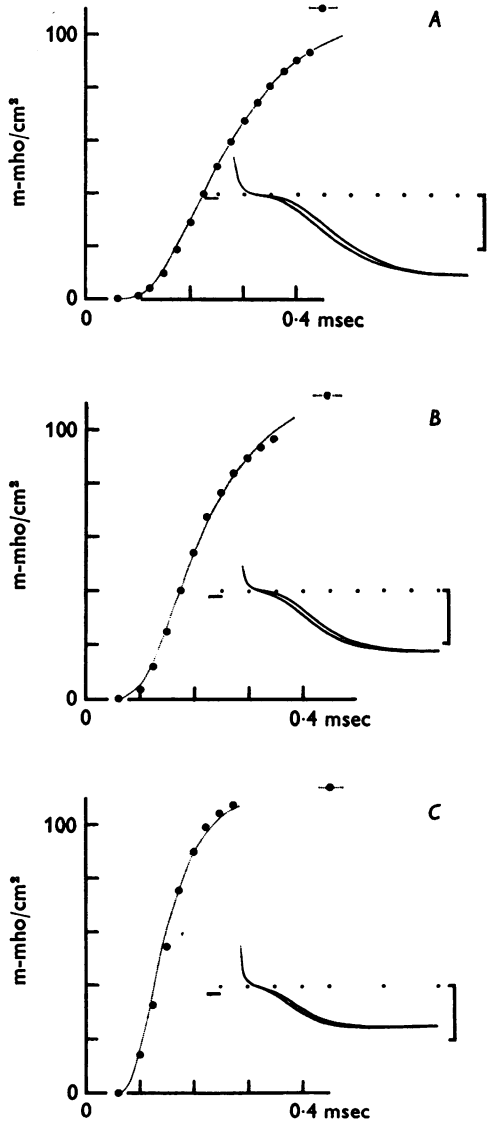

Fig. 4. The effect of holding potential on the initial delay in the rise of I_{Na}. Expt. 23–N-2, fibre perfused with high caesium in Na–SW at 8·7° C. The inserts show superimposed current traces recorded with voltage-clamp pulses taking the membrane potential from V_h − 90 or − 140 mV to V_p 30 mV (*A*), 50 mV (*B*), and 70 mV (*C*). The leakage current level is indicated by the series of points spaced 25 μsec apart; vertical calibration bar = 2 mA/cm². The points plotted on the left represent the sodium conductance divided by $\exp(-t/\tau_h)$ to correct for inactivation; V_h was − 140 mV in each case. $\bar{g}_{Na}$ was 110 m-mho/cm² in *A*, 112 in *B*, and 113 in *C*. The reversal potential for the early currents was 92 mV, making $P_{Na}/P_{Cs} = 30$. The lines represent the calculated time course of the conductance change if $g_{Na} = \bar{g}_{Na} m^3$ and δt = 50 μsec.

yielded not only the best fit for τ_m and δt, but also an objective estimate of the power to which the exponential term should be raised.

The effect on the early time course of I_{Na} of making the holding potential V_h increasingly negative is illustrated in Fig. 4. Each of the three inserts shows a pair of superimposed traces taken with the same value of V_p but with V_h first at -90 and then at -140 mV. At the more negative

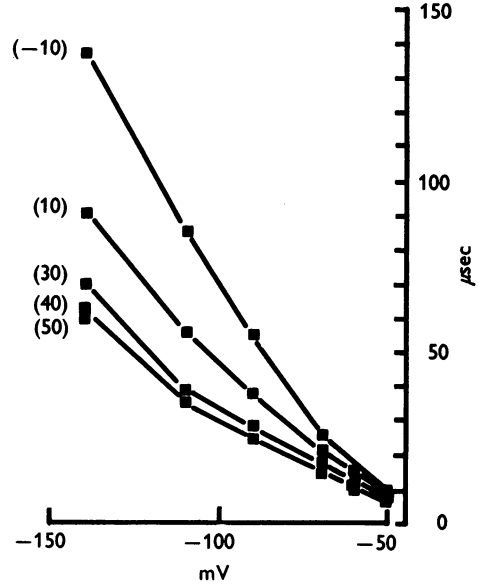

Fig. 5. The variation with V_p and V_h in the delay δt of the rise in the sodium conductance on depolarization. Ordinate: delay in μsec needed to fit the rise in I_{Na} to m^3 kinetics. Abscissa: holding potential in mV. Numbers in brackets against each curve indicate approximate value of V_p in mV. Results from expts. 23–N–2, 13–D–1, 20–D–1, 20–D–3, 18–D–1 and 18–D–2. Fibres were internally perfused with high caesium and bathed externally in ¼Na–SW.

holding potential the rise of I_{Na} was delayed by about 50 μsec without an obvious change in τ_m. Although the initial delay could be reproduced by taking $\delta t = 0$ and assuming m^8h kinetics instead of m^3h, this gave a very poor fit with the later part of the change in I_{Na}. The conclusion both from graphical tests and from the computer curve fitting was that m should always be raised to a power close to 3, and that the initial delay required the introduction of δt. On a number of occasions, the value of δt to give the best fit with the delay in the rise of I_{Na} was investigated systematically as a function of V_p and V_h and the results are shown in Fig. 5. It is seen that at a given holding potential, δt decreased as V_p became more positive, while for a constant V_p, the delay increased progressively as V_h became more negative. At the normal resting potential in the region of -60 mV where

Hodgkin & Huxley (1952*b*) worked, δt was only about 10 μsec, so that there is no real conflict with their data.

Temperature had a dramatic effect on δt. With $V_h = -100$ mV and $V_p = 0$ mV, δt was nearly 150 μsec at 4° C but less than 20 μsec at 16° C. The size of its Q_{10} in three axons was 7 ± 1. Since the Q_{10} is only 3 for τ_m (Hodgkin & Huxley, 1952*b*) and for the gating current time constant (Keynes & Rojas, 1974), the much larger Q_{10} of δt suggests that the delay induced by hyperpolarization involves an interaction with some part of the membrane other than the gating particles. It may be significant that the fast phase of the change in optical retardation of the membrane displays an equally large effect of temperature (Cohen, Hille, Keynes, Landowne & Rojas, 1971).

The values of τ_m between -60 and -140 mV were obtained from the I_{Na} transients during the turning off of sodium conductance on repolarization of the membrane. The I_{Na} tails pursued an exponential time course whose time constant $\tau_{Na,off}$ was determined from a semilogarithmic plot of the digitalized values of I_{Na}, only currents smaller than 0·6 mA/cm^2 being taken into account. These plots always had a single time constant, with no initial delay at any value of the potential. Again assuming m^3 kinetics to apply, $\tau_m = 3\,\tau_{Na,off}$. There were indications which have interesting implications and need further exploration that between -60 and -30 mV, τ_m may be appreciably greater for opening the sodium channels than for closing them.

For purposes of comparison with other data, it was necessary to plot τ_m as a function of the absolute membrane potential rather than the displacement in potential during the pulse, and to normalize all the results to a standard temperature of 6·3° C taking the Q_{10} as 3, in line with Hodgkin & Huxley (1952*b*). As may be seen from Fig. 6, the relation between τ_m and V was a nearly symmetrical bell-shaped curve whose maximum lay at -36 mV. The curve derived by Hodgkin & Huxley (1952*b*) to fit their results is shown as a dashed line. It has been plotted on the assumption that the average resting potential of their axons was the same as ours, that is -57 mV (Table 3), bringing its maximum to $-57+25 = -32$ mV. There was, on the whole, excellent agreement between the two sets of values, the divergence of the curves at large negative potentials having little significance, since they made rather few measurements over this range.

Steady-state properties of the sodium system

On a number of occasions, families of I–V curves were recorded with intact axons, first in normal Na–SW and then with I_{Na} reduced either by lowering the external sodium or by treatment with tetrodotoxin. After correcting as far as possible for the effect of incomplete compensation for

the series resistance R_s, the values of the following were calculated: (i) the reversal potential for the sodium current, V_{Na}; (ii) the peak sodium conductance, $\bar{g}_{Na}$; (iii) the midpoint of the m_∞ curve, that is the curve relating $\sqrt[3]{(g_{Na}/\bar{g}_{Na})}$ to potential; (iv) the depolarization required for an e-fold increase in g_{Na} at the steepest point of the g_{Na}–V curve. The results are given in Table 3. They suggest that with the full sodium current flowing, there was still a residual error from the uncompensated series resistance

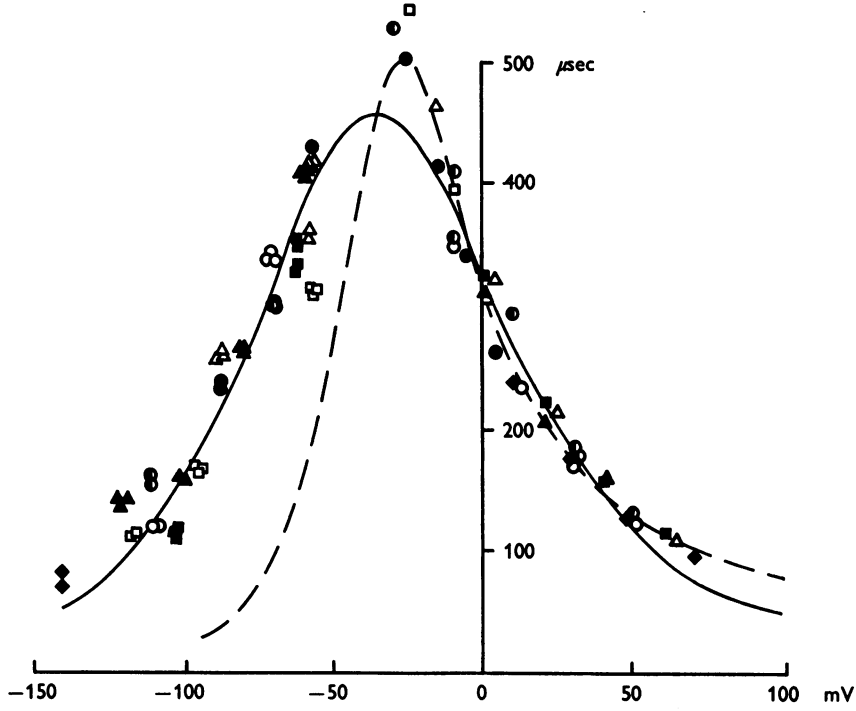

Fig. 6. The voltage dependence of τ_m. The experimental values were normalized to a standard temperature of 6·3° C, assuming a Q_{10} of 3. All fibres were perfused internally with high caesium, and bathed externally in ¼Na–SW. The continuous curve was computed as the least squares best fit with eqn. (12) in the form

$$\tau_m = \frac{1}{A \exp(BV) + C \exp(DV)}$$

with $A = 0{\cdot}00260 \pm 0{\cdot}000095\ \mu\text{sec}^{-1}$, $B = 0{\cdot}0254 \pm 0{\cdot}0016\ \text{mV}^{-1}$, $C = 0{\cdot}00040 \pm 0{\cdot}00006\ \mu\text{sec}^{-1}$, $D = -0{\cdot}0270 \pm 0{\cdot}0015\ \text{mV}^{-1}$, whence $kT/a = -19{\cdot}1$ mV, $V_0 = -36$ mV, $x = 0{\cdot}485$. The dashed line was calculated from eqns. (20) and (21) of Hodgkin & Huxley (1952*b*), taking the resting potential in their experiments as −57 mV.

○, 20D3, 7° C, $r_s = 4{\cdot}6\ \Omega\ \text{cm}^2$.
■, 20D1, 7° C, $r_s = 4{\cdot}6\ \Omega\ \text{cm}^2$.
▲, 13D1, 8° C, $r_s = 4{\cdot}6\ \Omega\ \text{cm}^2$.
◆, 23N2, 8·5° C, $r_s = 4\ \Omega\ \text{cm}^2$.
△, 21D2, 6·2° C, $r_s = 2{\cdot}5\ \Omega\ \text{cm}^2$.
●, 21D1, 7° C, $r_s = 4\ \Omega\ \text{cm}^2$.
◑, 18D1, 7·5° C, $r_s = 4{\cdot}6\ \Omega\ \text{cm}^2$.
□, 12D3, 10·5° C, $r_s = 4\ \Omega\ \text{cm}^2$.

TABLE 3. Steady-state properties of the sodium system measured in non-perfused fibres

Expt. no.	$[Na]_o$ (mM)	$[TTX]_o$ (nM)	Resting potential (mV)	Holding potential V_h (mV)	Na reversal potential V_{Na} (mV)	Maximum Na conductance $\bar{g}_{Na}$ (m-mho/cm²)	R_s (Ω cm²)	r_s (Ω cm²)	Midpoint of the $\sqrt[3]{\left(\frac{g_{Na}}{\bar{g}_{Na}}\right)}$ vs. V_p curve (mV)	Potential for an e-fold change in g_{Na} (mV)	Temp. (°C)
4–0–2†	430	0	−55	−70	52	55	3·2 ×	3·2	−27	6·0	8·2
	215	0	−52	−70	36	36			−25	6·5	8·7
	107·5	0	−51	−70	19·5	22			−19*	6·7*	8·5
22–N–1	460	0	−58	−65	44·5	106	5·0	3·0	−32	6·2	14·5
(1971)	345	0	−59	−65	38	97			−29	6·5	14·0
	200	0	−60	−65	26	58			−26·5	6·75	14·0
	100	0	−61	−65	11	28			−24*	7·0*	14·0
27–N–2	460	0	−55	−60	52	73	3·3	2·0	−27·4	6·1	16·5
(1971)	345	0	−56	−60	47·5	71·6			−26·5*	6·2*	16·0
	460	5	−53	−60	51·5	20·5			−26·5*	6·8*	16·0
16–N–2	460	0	−55	−60	45	84	3·4	3·4	−27·5	5·2	16·0
(1971)	460	50	−55	−60	45	6			−24*	7·0*	15·5
22–N–2	460	0	−56	−65	50	84·5	4·9	4·0	−39	5·0	13
	460	25	−55	−65	50	22			−27·5*	6·25*	13
	345	0	−51	−65	31	80			−26*	6·5*	13
3–D–2	460	0	−66	−70	56	88·5	2·6	2·6	−31	5·2	4·5
(1971)	230	0	−65	−70	43	36·9			−29*	6·0*	4
	460	18	−64	−70	56	6·7			−25*	6·0*	18·5
						Mean ± S.E. of asterisked values			−25·3 ± 1·0	6·5 ± 0·1	

R_s = measured series resistance, except in cases marked × where it was estimated from data in Table 2.

r_s = amount of compensation for series resistance, measured as the ratio of the displacement of the membrane potential from the commanded level to the peak inward current flowing during the pulse, I_m. I–V curves were corrected by adding $I_m (R_s - r_s)$ to the measured pulse potentials.

† This experiment was performed in a different nerve chamber designed to minimize fringe effects, similar to that described by Armstrong, Bezanilla & Rojas (1973).

$R_s - r_s$, since both methods of cutting down I_{Na} consistently increased the potential for an e-fold change in g_{Na} and shifted the midpoint potential in a positive direction. Thus reduction of I_{Na} increased the mean potential for an e-fold change from $5{\cdot}6 \pm 0{\cdot}2$ mV in normal Na–SW to $6{\cdot}5 \pm 0{\cdot}1$ MV, and at the same time shifted the midpoint potential from $-30{\cdot}7 \pm 1{\cdot}9$ to $-25{\cdot}3 \pm 1{\cdot}0$ mV. The most reliable determinations of these two parameters would therefore seem to be those made with the smallest I_{Na}, yielding the averages shown in Table 3.

Before conducting the gating current runs on perfused axons, I–V curves were recorded in $\frac{1}{4}$Na–SW, and after correction for incomplete compensation, the same parameters were determined. In Fig. 7 the resulting values of m_∞, again calculated as $\sqrt[3]{(g_{Na}/\bar{g}_{Na})}$, have been plotted against potential. A difficulty is encountered in fitting the symmetrical function of p. 179 $[1 + C/A \exp{(D-B)V}]^{-1}$, to the points, since a good fit cannot be obtained simultaneously at both ends of the curve. Assuming the values for the smaller pulses to be the most reliable, the solid line is obtained, with a midpoint falling at -34 mV, and a slope at this point (which is $-\frac{1}{4}(D-B) = -a/4kT$) of $0{\cdot}0139\ \text{mV}^{-1}$. The dashed line calculated for the whole array of points has its midpoint at -32 mV, but a slope of $0{\cdot}0200\ \text{mV}^{-1}$.

Some while after these computations had been completed, the question was raised whether for the perfused axons employment of the conductance formulation $g_{Na} = I_{Na}/(V - V_{Na})$ was justified, as it is for intact axons (Hodgkin & Huxley, 1952*a*; Bezanilla, Rojas & Taylor, 1970), by linearity of the instantaneous I–V curve. We have not yet had an opportunity to check the instantaneous I–V relationship in axons perfused with caesium fluoride, but Fig. 8 shows that a plot of peak initial current against potential departs from linearity as it approaches the reversal potential in much the same way as it does at the node of Ranvier (Dodge & Frankenhaeuser, 1959), presumably because of the low concentration of ions in the membrane when the current is flowing outwards through the sodium channels. When, therefore, m_∞ is calculated as $\sqrt[3]{(g_{Na}/\bar{g}_{Na})}$, it reaches its peak at about $+10$ mV, but for more positive potentials it falls off again. If, instead, m_∞ is calculated as $\sqrt[3]{(P_{Na}/\bar{P}_{Na})}$, where P_{Na} is the sodium permeability coefficient of the membrane in the constant field relationship

$$P_{Na} = I_{Na} \frac{RT}{F^2 V} \frac{1}{[Na]_o} \frac{\exp\{VF/RT\} - 1}{\exp\{(V - V_{Na})F/RT\} - 1}$$

(Dodge & Frankenhaeuser, 1959), and $\bar{P}_{Na}$ is its value when V is large and positive, the m_∞ curve attains a satisfactorily level plateau. At least under the conditions of these measurements, it would seem that the state of the membrane is better described by P_{Na} than by g_{Na}.

In view of this conclusion, m_∞ should ideally have been derived throughout from P_{Na} rather than g_{Na}. However, it was impracticable to reprocess all the data from the I–V curves, and it must suffice for the present to consider the probable effect on the averaged m_∞ curve shown in Fig. 7 of

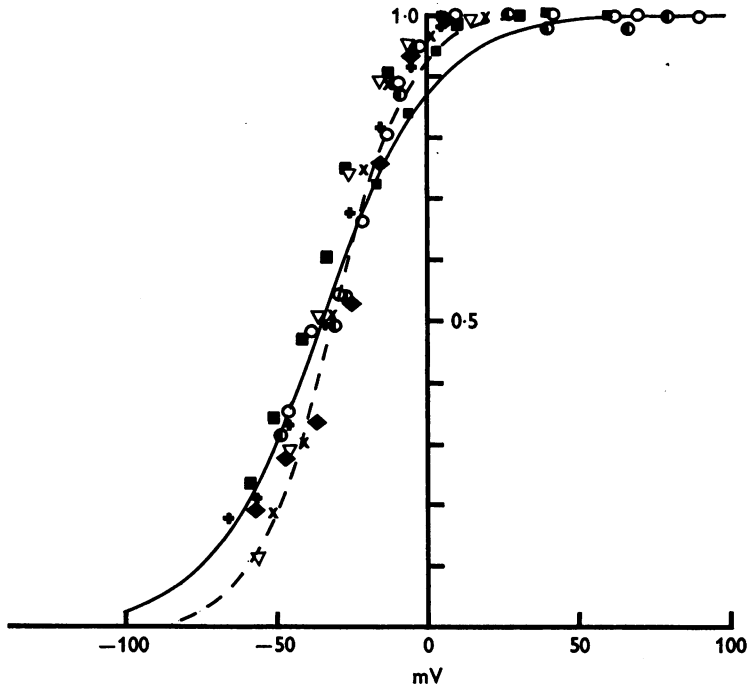

Fig. 7. The voltage dependence of m_∞ for perfused fibres bathed in ¼Na–SW. All experimental points were calculated as explained in the text on the assumption that m^3h kinetics were followed. The continuous curve was computed to give a least-squares best fit with the values of m_∞ for potentials between −70 and −20 mV, using eqn. (17) in the form

$$m_\infty = \frac{1}{1+C/A \exp{(D-B)V}}.$$

This gave $C/A = 0{\cdot}150 \pm 0{\cdot}009$, and $(D-B) = -0{\cdot}0555 \pm 0{\cdot}0062$ mV^{-1}, whence $kT/a = -18{\cdot}0$ mV and $V_0 = -34$ mV. The dashed curve was computed for all the points, leading to $C/A = 0{\cdot}080 \pm 0{\cdot}007$ and $(D-B) = -0{\cdot}0801 \pm 0{\cdot}0091$ mV^{-1}, whence $kT/a = -12{\cdot}5$ mV and $V_0 = -32$ mV. Fibres internally perfused with high caesium −1 and bathed in ¼Na–SW made with chloride: ◑, 18D1, $V_h = -60$ and -100 mV, $V_{Na} = 78$ mV; ■, 20D1, $V_h = -60$ and -100 mV, $V_{Na} = 76$ mV; ○, 20D3, $V_h = -50$ and -90 mV, $V_{Na} = 77$ mV. Fibres internally perfused with high caesium −2 and bathed in ¼Na–SW made with isethionate and 15 mM caesium: ×, 10J2-75, $V_h = -100$ mV, $V_{Na} = 94$ mV; ◆, 11J2–75, $V_h = -95$ mV, $V_{Na} = 95$ mV; ▽, 16J1-75, $V_h = -95$ mV, $V_{Na} = 95$ mV; +, 16J3–75, $V_h = -85$ mV, $V_{Na} = 95$ mV.

using values recomputed on a P_{Na} basis. As may be seen in Fig. 8, the principal differences between the new and old m_∞ curves are a shift of about 5 mV in the midpotential, and the elimination of the droop in m_∞ in the positive potential range. Hence the revised value for the midpotential would be in the region of -29 mV. This is satisfactory in that it reduces the discrepancy between perfused and intact axons, checks having shown

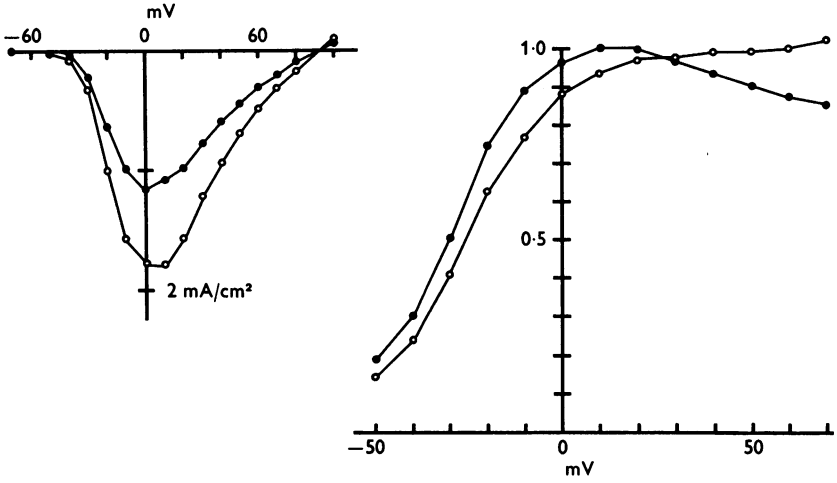

Fig. 8. Calculation of m_∞ from P_{Na} instead of g_{Na}. The left-hand graph shows I–V curves with values of peak I_{Na} corrected for leakage currents only, ●, and of I_{Na}^{∞} corrected also for inactivation, ○. The right-hand graph shows m_∞ calculated as described in the text from g_{Na}, ●, and from P_{Na}, ○. Experiment 10J2-75. Fibre perfused with high caesium -2 and bathed in ¼Na–SW made with isethionate in place of chloride. Holding potential -100 mV. Temperature 5° C.

that for the latter the value of m_∞ is much the same whichever basis is used for its calculation. It is also evident that the asymmetrical distribution of the plotted points in Fig. 7 can be attributed to a combination of the droop in m_∞ with the instructions given to the computer to use the value for $V = +20$ mV for purposes of normalization.

Steady-state properties of the gating system

After making the voltage-clamp runs in ¼Na–SW just described, the external solution was replaced by Tris–SW containing tetrodotoxin. With the sodium current thus blocked, it was readily possible to record the asymmetrical displacement currents for various potential steps from holding potentials ranging from -140 to $+50$ mV, either in single sweeps with high current amplifier gain, or using a signal averager for summation

of the currents for equal and opposite pulses. Some typical traces are illustrated in Fig. 9. The holding potential was -60 mV throughout, and the applied pulses were ± 60 mV in *A* and ± 80 mV in *B*. The upper records show the rates of turning on and off I_{Na} for the corresponding values of V_p at the same V_h. The single sweep records in the middle show the displacement currents remaining when the same pulses were applied after abolishing the sodium current. The lower part of the Figure shows the net displacement current after signal averager summation.

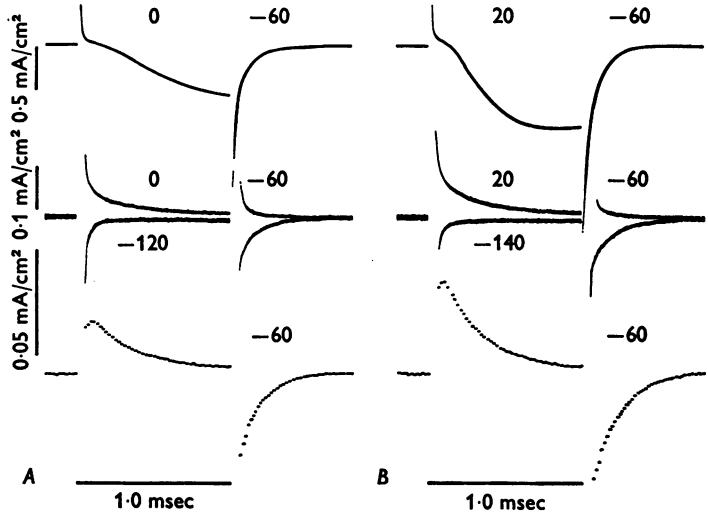

Fig. 9. Comparison between sodium inward currents and asymmetrical displacement currents. The fibre was first perfused with high caesium and bathed in ¼Na–SW; the series resistance compensation r_s was 4·6 Ω cm². At this time the records shown in the upper part were made. Next, the ¼Na–SW was replaced by Tris–SW made with 300 nM tetrodotoxin and isethionate as main anion, and in this solution the single sweep displacement current records shown in the middle traces were made. The traces in the lower part are the signal averager records of the sum of 300 pairs of the transients shown above. The figures against the traces show the membrane potentials during and between pulses in mV. Experiment 20–D–3.

We have previously (Keynes & Rojas, 1974; Rojas & Keynes, 1975) analysed the steady-state arrangement of the mobile charges in terms of a Boltzmann distribution with two allowed configurations whose energies are ϵ_1 and ϵ_2. It can be shown that for large negative values of V_h the energy difference between these states is given by

$$\Delta\epsilon = \epsilon_1 - \epsilon_2 = kT \ln \frac{q(V_p, \infty)}{Q_{max} - q(V_p, \infty)}, \qquad (3)$$

where $q(V_p, \infty)$ is the charge transferred during a long pulse taking the potential to a level V_p, and Q_{max} is the charge transferred when V_p is sufficiently large and positive for saturation to be reached (Rojas & Keynes, 1975). In Fig. 10 the right hand side of eqn. (3) has been plotted on a logarithmic scale against absolute membrane potential for an experiment in which V_h was -100 mV and V_p was taken up to $+80$ mV. The points are reasonably well fitted by a straight line, from which we may conclude that for our present purpose Boltzmann's Law provides an adequate description of the steady-state behaviour of the gating particles,

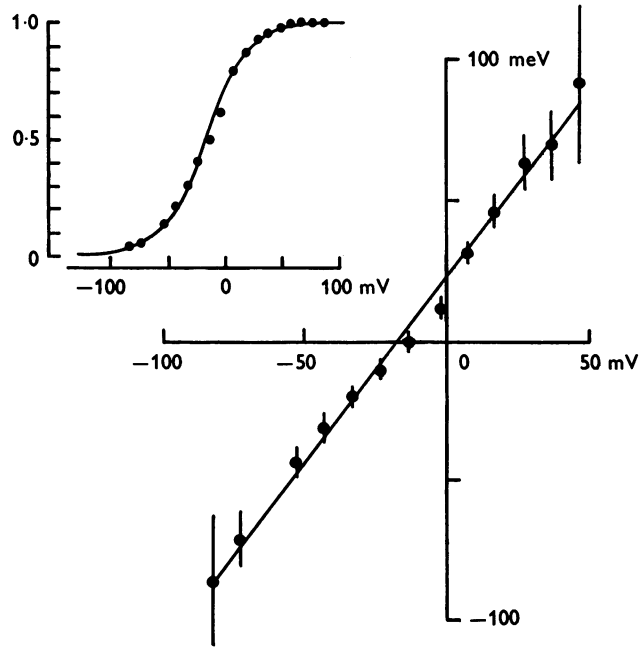

Fig. 10. The steady-state distribution of the charges, and evaluation of the energy difference $\epsilon_1 - \epsilon_2$. The vertical bars drawn through the points represent approximate values of the total derivative of eqn. (3) for a maximum error of 5% in the determination of $q(V_p, \infty)/Q_{max}$. The straight line is the least-squares regression line. The charge displaced during the pulses, $q(V_p, \infty)$, was estimated from single-sweep current transients recorded at high gain. Q_{max} was reached at an absolute membrane potential of about 50 mV, and amounted to 31 nC/cm^2. Expt. 3001. The fibre was internally perfused with low caesium, and bathed in Tris–SW made with isethionate in place of chloride. From the regression line, $kT/a = -20{\cdot}2$ mV and $V_0 = -19$ mV.

The insert shows the same data, plotted as the fraction of the charges that underwent the transition from one energy state to the other. The line shows the distribution calculated from Boltzmann's Law, using the same parameters.

and that at least between -100 and $+80$ mV the energy difference can be treated as a linear function of the transmembrane potential. Writing

$$\epsilon_1 - \epsilon_2 = aV_0 - aV, \tag{4}$$

the intercept on the potential axis yields the value of V_0, which may be termed the transition potential. The slope a of the line may be equated with the effective valency of the individual gating particles. For the case illustrated, V_0 was -17 mV and a was $-1{\cdot}3$; these values were used for calculation of the curve drawn in the insert. As may be seen in Fig. 15 of Keynes & Rojas (1974), similar plots were simply shifted laterally by alterations in surface potential brought about by lowering the internal ionic strength or changing the external calcium concentration, so that under these experimental conditions V_0 was changed but a was not.

Fig. 11 shows the equilibrium distribution of the gating particles plotted against potential for a number of fibres perfused with high caesium. The average value of the midpoint potential was -26 mV, which has to be compared with about -29 mV for the m_∞ curves calculated from P_{Na} for the same perfused axons, and with -25 mV for the m_∞ curves calculated from g_{Na} for the intact axons. Since there is inevitably some residual uncertainty over the exact magnitude of the junction potentials that obtained in each set of measurements, and over the difference in V_0 to be expected between perfused and intact axons, the agreement seems rather good. Nevertheless, it is not impossible to conceive reasons why the mid-potentials should not be quite identical, and the results do not rule out the existence of some genuine slight displacements between the several curves.

The average value of Q_{max} for the axons of Fig. 11 was 34 nC/cm^2, or 2114 e/μm^2. Since kT/a was $-18{\cdot}5$ mV for the individual charged particles, the total charge carried by three such particles would be 4 e. The estimated density of sodium channels was therefore 530 μm^{-2}. Both Levinson & Meves (1975) and Keynes *et al.* (1975) obtained figures of the same order of magnitude for the number of tetrodotoxin binding sites, as did Conti, de Felice & Wanke (1975) from their measurements of the sodium current noise spectrum.

It should be noted in this connexion that the difference in shape of the steady-state charge distribution curves predicted on the one hand for a Boltzmann system with only two permitted energy states, and on the other for a system with a continuous distribution of energies, e.g. the Langevin–Debye function, is probably not great enough to establish unequivocally that the model we have chosen is the correct or only one. Although it may be felt intuitively that a two-state model is the more likely to be valid, we cannot on the present evidence rule out the

possibility that the system should really be regarded as one with two restricted ranges of energy states, whose behaviour would be intermediate between Boltzmann and Langevin–Debye.

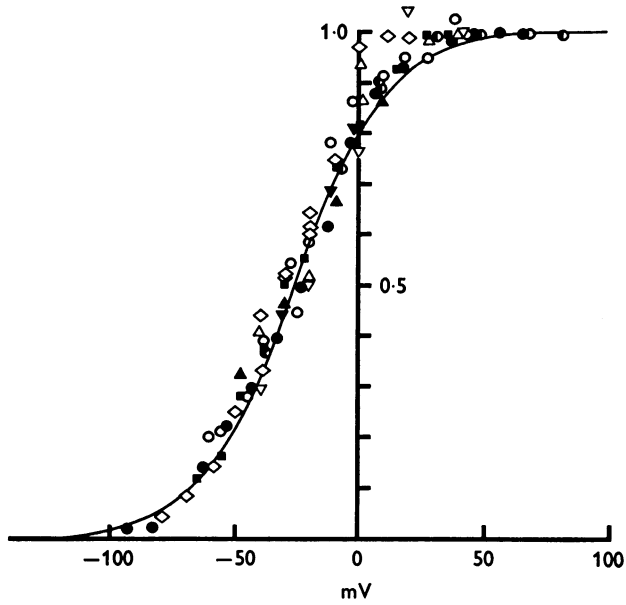

Fig. 11. The voltage dependence of the steady-state distribution of the mobile charges. In all cases the fibres were bathed in Tris–SW containing isethionate in place of chloride. The curve was computed as the least-squares best fit with eqn. (17), giving $C/A = 0{\cdot}245$ and $(D-B) = -0{\cdot}054\ \mathrm{mV}^{-1}$, and hence $kT/a = -18{\cdot}5$ mV and $V_0 = -26$ mV. Fibres internally perfused with high caesium: ◑, 18D1, $V_h = -100$ mV, $Q_{max} = 40$ nC/cm²; ■, 20D1, $V_h = -100$ mV, $Q_{max} = 29$ nC/cm²; ○, 20D3, $V_h = -90$ mV, $Q_{max} = 32$nC/cm²; ▲, 13D1, $V_h = -100$ mV, $Q_{max} = 47$ nC/cm²; ▼, 23N2, $V_h = -91$ mV, $Q_{max} = 30$ nC/cm²; △, 11D3, $V_h = -100$ mV, $Q_{max} = 31$ nC/cm²; ▽, 12D2, $V_h = -100$ mV, $Q_{max} = 37{\cdot}5$ nC/cm². Fibres internally perfused with low caesium, and experimental points shifted by 9 mV in a negative direction: ◇, 20N3, $V_h = -100$ mV, $Q_{max} = 20$ nC/cm²; ●, 30O1, $V_h = -103$ mV, $Q_{max} = 40$ nC/cm².

Kinetic properties of the gating system

During a given potential step, a rearrangement of the charges takes place that continues in time until a new equilibrium distribution is achieved. The evidence presented earlier (Keynes & Rojas, 1974; Rojas & Keynes, 1975; Nonner *et al.* 1975) that the asymmetrical displacement current follows an exponential time course characterized by a single time constant suggests rather strongly that the charge displacement is a first

order process. In order to examine its voltage dependence, we shall assume for the sake of simplicity that the system can be regarded as a two-state one in which the charges have to traverse a single energy barrier separating two energy wells. Provided that the density of the mobile charges is low enough for the height of the energy barrier to be unaffected by their passage, it can be shown that the rate constants are exponential functions of the energy difference between the top of the barrier and the level from which the charges are being displaced (Glasstone, Laidler & Eyring, 1941). It follows (see Rojas & Keynes, 1975, for a fuller treatment) that the rate constants α and β for the transition may be written as

$$\alpha = \theta \exp\left(\frac{\epsilon_1 - \epsilon_b}{kT}\right), \tag{5}$$

$$\beta = \theta \exp\left(\frac{\epsilon_2 - \epsilon_b}{kT}\right), \tag{6}$$

where θ is a constant and ϵ_b is the height of the energy barrier. Hence

$$\frac{\alpha}{\beta} = \exp\left(\frac{\epsilon_1 - \epsilon_2}{kT}\right), \tag{7}$$

$$= \exp\left\{\frac{a}{kT}(V_0 - V)\right\}, \tag{8}$$

where V_0 is, as in eqn. (4), the potential at which ϵ_1 and ϵ_2 are equal. Assuming that

$$\epsilon_b = \epsilon_0 - ax(V_0 - V), \tag{9}$$

where x is a fraction determined by the symmetry of the system and ϵ_0 is a reference energy level, then

$$\epsilon_1 - \epsilon_b = \epsilon_1 - \epsilon_0 + ax(V_0 - V), \tag{10}$$

$$\epsilon_2 - \epsilon_b = \epsilon_1 - \epsilon_0 - a(1-x)(V_0 - V). \tag{11}$$

Hence the gating current time constant $\tau(V)$ is given by

$$\tau(V) = \frac{1}{\alpha + \beta},$$

$$= 1/\left[\theta \exp\left\{\frac{\epsilon_1 - \epsilon_0 + axV_0}{kT}\right\} \exp\left\{\frac{-ax}{kT} V\right\}\right.$$

$$\left. + \theta \exp\left\{\frac{\epsilon_1 - \epsilon_0 - a(1-x)V_0}{kT}\right\} \exp\left\{\frac{a(1-x)}{kT} V\right\}\right], \tag{12}$$

so that if the function $1/[A \exp(B)V + C \exp(D)V]$ is fitted to the data for $\tau(V)$, then

$$D - B = \frac{a}{kT}, \tag{13}$$

$$\frac{B}{B-D} = x, \tag{14}$$

$$\frac{A}{C} = \exp \frac{a}{kT} V_0. \tag{15}$$

Also, from (3) and (7),

$$\frac{q(V_p, \infty)}{Q_{max}} = \frac{\alpha}{\alpha+\beta}, \tag{16}$$

$$= \frac{1}{1+\exp\{(-a/kT)(V_0 - V)\}},$$

$$= \frac{1}{1+(C/A)\exp(D-B)V}. \tag{17}$$

From measurements of $\tau(V)$ and $q(V_p, \infty)/Q_{max}$, the rate constants at a given potential can be individually evaluated. In Fig. 12 the values of α and β for the experiment of Fig. 10 have been plotted on a logarithmic scale against potential. Both sets of points fall reasonably well on straight

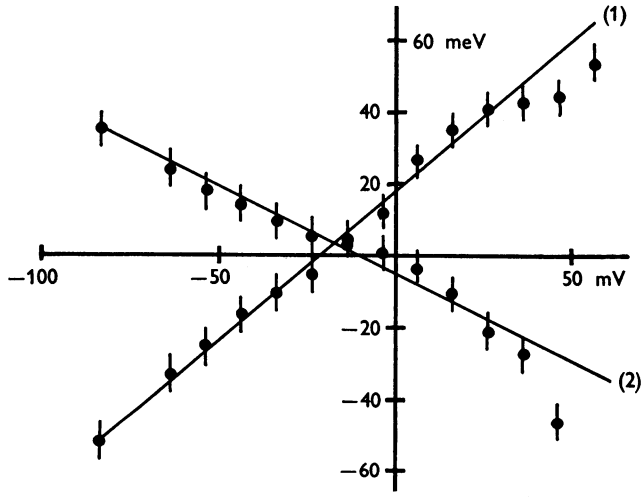

Fig. 12. The voltage dependence of the individual rate constants for the experiment of Fig. 10. Ordinate: (1) $kT \ln \alpha$, (2) $kT \ln \beta$, in meV. Abscissa: membrane potential in mV. The least-squares regression lines gave

$$kT \ln \theta + (\epsilon_1 - \epsilon_b) = 18 + 0{\cdot}82V,$$

$$kT \ln \theta + (\epsilon_1 - \epsilon_b) = -4{\cdot}5 - 0{\cdot}38V.$$

lines, which argues in favour of the validity of the model on which eqns. (5), (6), (10) and (11) are based. In other words, the charges do behave as if they encounter a single energy barrier whose height is linearly dependent on the membrane potential, at least over the physiological range between -70 and $+50$ mV. While further support for a model of this type is provided by the observations of Ketterer, Neumcke & Läuger (1971) on the passage of hydrophobic ions through lipid bilayers, an alternative that deserves at least passing consideration would be a constant field system. Preliminary calculations suggest that although on a constant field basis α and β would no longer exhibit a simple exponential dependence on potential, it would nevertheless be premature to conclude that some compromise between single and multiple energy barriers can definitely be ruled out.

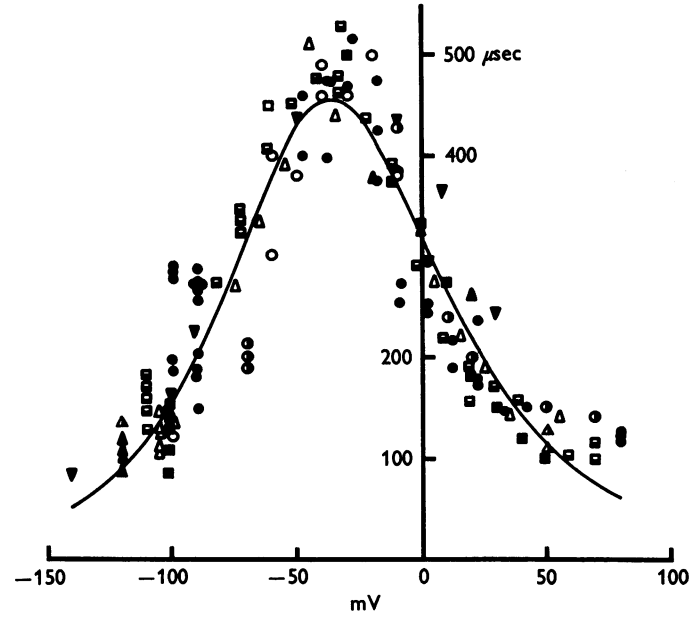

Fig. 13. The voltage dependence of the gating current relaxation time constants. For potentials more positive than -50 mV, $\tau(V)$ was measured at the onset of the pulses, and V_p was varied. For more negative potentials, $\tau(V)$ was measured during the tail of the gating current, and V_h was varied. All results were normalized to a standard temperature of 6·3° C, taking the Q_{10} as 3. The line was computed as the least-squares best fit with eqn. (12), the parameters being: $A = 0{\cdot}00276 \pm 0{\cdot}00015$ μsec^{-1}; $B = 0{\cdot}0224 \pm 0{\cdot}0021$ mV^{-1}; $C = 0{\cdot}00034 \pm 0{\cdot}00008$ μsec^{-1}; $D = -0{\cdot}0289 \pm 0{\cdot}0027$ mV^{-1}. Hence $kT/a = -19{\cdot}5$ mV, $V_0 = -41$ mV, $x = 0{\cdot}44$. Fibres perfused with high caesium: ○, 20D3, 7° C; ■, 20D1, 6·4° C; ▲, 13D1, 8° C; ▼, 23N2, 8·5° C; △, 21D2, 6·2° C; ◑, 18D2, 7·5° C. Fibres perfused with low caesium, points plotted with membrane potentials shifted 9 mV in a negative direction; ◭, 23O2, 6·2° C; ⬓, 30O1, 5·8° C. ●, values of $\tau(V)$ taken from Table 3 of Keynes & Rojas (1974).

Fig. 13 presents 132 values for $\tau(V)$ measured in twenty-five different fibres perfused with either low caesium, high caesium or high potassium. The curve drawn through the points is of the form of eqn. (12), and was computed for a least-squares best fit. Using eqns. (13), (14) and (15) it is found that $kT/a = -19{\cdot}5$ mV, $V_0 = -41$ mV, and $x = 0{\cdot}44$. Since the curve is thus slightly asymmetrical, its peak is displaced from V_0 by 5 mV in a positive direction, falling at about -36 mV. Although between about -100 and $+50$ mV eqn. (12) fitted the data reasonably well, there were indications that for potentials beyond these limits $\tau(V)$ did not continue to decrease as predicted, but instead reached a plateau at around 80 μsec. The system thus behaves as if it saturates, though this takes place only well outside the range over which it normally operates.

Comparison between Figs. 6 and 13 shows that both in absolute magnitude and in their voltage dependence, τ_m and $\tau(V)$ are in good agreement, each with their maximum in the neighbourhood of -36 mV. This means, however, that the values of V_0 obtained from the two sets of time constant measurements differ by about 10 mV from those derived from the m_∞ and steady-state charge distribution curves, a discrepancy for which, if it is genuine, there is no easy explanation. Nevertheless, the uncertainties in measuring the time constants for large negative values of V that arise from the effects of pulse size and holding potential (see below) may well have introduced a negative bias in both curve fitting operations. The scatter of the results is such that the true maxima of the τ_m and $\tau(V)$ curves could really be located close to -30 mV.

In connexion with the determination of $\tau(V)$, a caveat must be entered concerning errors that may arise from the addition of time-dependent leakage currents to the gating currents, especially when carrying out signal averager summation of the displacement currents for equal and opposite voltage-clamp pulses. Fig. 14 illustrates a series of single sweep records of the displacement current flowing on application of voltage-clamp pulses varying in size from $\pm 52{\cdot}5$ to ± 141 mV. Inspection of the traces for the hyperpolarizing pulses shows that for pulses smaller than about 110 mV the rapid capacity transient was followed by a slowly declining inward current. At 127·5 mV the amplitude of this component was zero, but at 141 mV it reappeared with its time dependence reversed, that is to say it now increased with time. This slowly increasing inward current was definitely greater in fibres bathed with solutions containing chloride as the principal anion than when chloride was replaced by isethionate, and may therefore have been an anionic leakage current. In the presence of such time-dependent leakage currents, summation of the records with a signal averager may yield apparent time constants up to 20% greater for small pulses, or 20% smaller for large ones, than those

of the single-sweep traces for depolarizing pulses measured separately. In experiments in which averaged hyperpolarizing transients are scaled up and down before being subtracted from the depolarizing transient to eliminate the symmetrical capacity current, it will clearly be necessary to beware of this source of error.

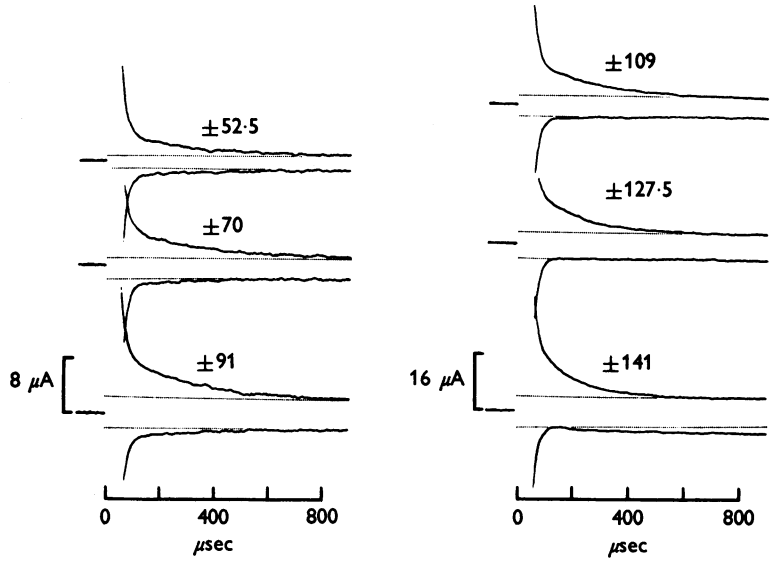

Fig. 14. Asymmetrical membrane currents showing time-dependent leakage components during hyperpolarizing pulses. Expt. 13–D–1; fibre internally perfused with high caesium in Tris–SW plus tetrodotoxin at 8° C. V_h = −100 mV. The size of the voltage-clamp pulses in mV is shown above the corresponding records. Current amplifier high frequency cut-off point set at 30 kHz.

DISCUSSION

The excellent agreement reported here between the properties of the gating currents and those of the sodium conductance treated as a system obeying m^3 kinetics (Hodgkin & Huxley, 1952*b*), fully confirms our previous conclusion (Keynes & Rojas, 1974) that the mobile charges responsible for generation of the asymmetrical components of the displacement current can be identified with the sodium gating particles. It might, of course, be a pure coincidence that the curves in Figs. 6 and 13, and in Figs. 7 and 11, should be so similar both in shape and in their position on the voltage axis, but this does not seem very likely. Remembering also that the total charge transfer fits nicely with estimates of the total number of tetrodotoxin binding sites (Keynes & Rojas, 1974; Levinson & Meves, 1975; Keynes *et al.* 1975), the simplest explanation is to accept that we

are indeed observing the movements of Hodgkin & Huxley's (1952*b*) previously hypothetical 'm' particles.

It is also satisfactory to be able to provide fresh and independent confirmation for the conclusion that, at least in the squid giant axon, the sodium conductance rises and falls according to a cube law. Thus, after making due allowance for inactivation, and introducing an initial time delay δt at large values of V_h, the time course of the rise in g_{Na} on depolarization fitted

$$g_{Na} = \bar{g}_{Na} m^3 \tag{18}$$

better than an expression incorporating either m^2 or m^4, as Hodgkin & Huxley (1952*b*) had shown. The original argument resting on a study of conductance kinetics can now be re-examined by comparing the voltage-dependence of g_{Na} with that of the gating particle distribution. Differentiation of eqn. (18) with respect to V leads at once to

$$\frac{1}{g_{Na}} \frac{d}{dV} (g_{Na}) = 3 \frac{1}{m} \frac{d}{dV} (m), \tag{19}$$

from which it is apparent that the limiting slope of a logarithmic plot of g_{Na} against potential should be three times greater than for m. Our best estimate for the relationship between g_{Na} and V was that at the steepest point an e-fold change in conductance was brought about by a 6·5 mV change in potential (Table 3), while for the steady-state charge distribution curve the limiting slope of a logarithmic plot, that is to say the value of kT/a determined as in Fig. 11, was $-18{\cdot}5$ mV. The slope ratio was therefore $18{\cdot}5/6{\cdot}5 = 2{\cdot}85$, close to the prediction of eqn. (19). It should be appreciated that it is the slopes for the smallest values of g_{Na} and m that have to be compared, not the slopes at the midpoints of the curves, for it is easy to show that when the m_∞ curve is cubed, the effect is simply to displace its midpoint by about 25 mV towards a more positive potential, but that at this point the m_∞^3 curve is not much steeper than the m_∞ curve. Another way of testing the validity of eqn. (18) is to compare the curves for the cube roots of $g_{Na}/\bar{g}_{Na}$ and $P_{Na}/\bar{P}_{Na}$ in Figs. 7 and 8 with that for the charge distribution in Fig. 11. Not only is there reasonable agreement between their positions on the voltage axis, but they have very similar slopes ($= -a/4kT$) at their midpoints, in each case just under 0·014 mV^{-1}.

At the node of Ranvier, it has been shown by Frankenhaeuser (1960) that m^2 rather than m^3 kinetics fits the data best. Nonner *et al.* (1975) found that the steady-state distribution curve for the gating particles was somewhat steeper than in squid, the value of kT/a being $-14{\cdot}9$ mV; but the sodium conductance increased less steeply, with an e-fold change for 7·1 mV. The slope ratio was therefore $14{\cdot}9/7{\cdot}1 = 2{\cdot}1$. Once again the conductance kinetics and gating current approaches are in good agreement,

but it would appear that whereas in squid each sodium channel behaves as if it was controlled by three gating particles, at the node of Ranvier the number is only two.

Although, as we have shown, the initial rise in the sodium conductance can be delayed by as much as 100 μsec at 6° C if the holding potential is raised to -150 mV, there was no evidence for the occurrence of a comparable delay in the gating current. In many of our experiments, however, a switching pulse was applied in order to prevent overloading of the current amplifier and signal averager during the first 50 μsec (Armstrong & Bezanilla, 1973; Keynes & Rojas, 1974), and under these conditions a delay in the onset of the gating current would not have been seen. There was also no evidence, regardless of the value of the holding potential on repolarization, that the turning off of the sodium conductance was delayed at the end of the pulse. The nature of the delay suggests that the opening of the sodium channels involves a second process operating in series rather than in parallel with the gating particles, but there is no evidence as to what this process might be. The fast phase of the optical retardation response described by Cohen *et al.* (1971) has a relaxation time of the order of magnitude of the delay with the same very large Q_{10}, but unfortunately it is not yet known what underlying molecular rearrangement is involved, and we can only make the tentative suggestion that the two phenomena may somehow be connected.

Several features of the findings on gating currents reported previously appeared to be in direct conflict with the identification of the mobile charges with the sodium gating particles, and must therefore be examined further. Thus it was originally stated both by ourselves (Keynes & Rojas, 1974) and by Bezanilla & Armstrong (1975) that the time constant for turning off the sodium conductance at the end of a brief depolarizing pulse, $\tau_{Na,off}$, was nearly equal to the gating current time constant, $\tau(V)_{off}$, instead of being the predicted one third as great. It has also been clear from the start (Keynes & Rojas, 1974; Meves, 1974) that $\tau(V)$ is not always, as it should be according to our theoretical treatment, determined solely by the new value of the membrane potential, for on repolarization to a constant value of V_h, $\tau(V)_{off}$ was not independent of V_p, but increased both with pulse size and with pulse duration. Further confirmation of this behaviour is presented in Fig. 15. Yet Hodgkin & Huxley (1952*b*) did not observe any variation of $\tau_{Na,off}$ with pulse size, so that even if an explanation can be found for the dependence of $\tau(V)_{off}$ on V_p, there is still a difficulty in fixing $\tau_{Na,off}$ in relation to $\tau(V)_{off}$, whether at one third or any other fraction. Another problem is to account for the differential action of heavy water, which slows down the sodium conductance time constants without affecting the gating current time constants (Meves, 1974).

We present in Table 4 five sets of parallel measurements of $\tau_{Na,off}$ and $\tau(V)_{off}$ in the same three axons. In determining $\tau_{Na,off}$, particular attention was paid to the prolongation of the time constant that would be caused by incomplete compensation for the series resistance, which was countered both by introducing as much electrical compensation as possible, and by lowering the external sodium concentration so as to reduce I_{Na} to

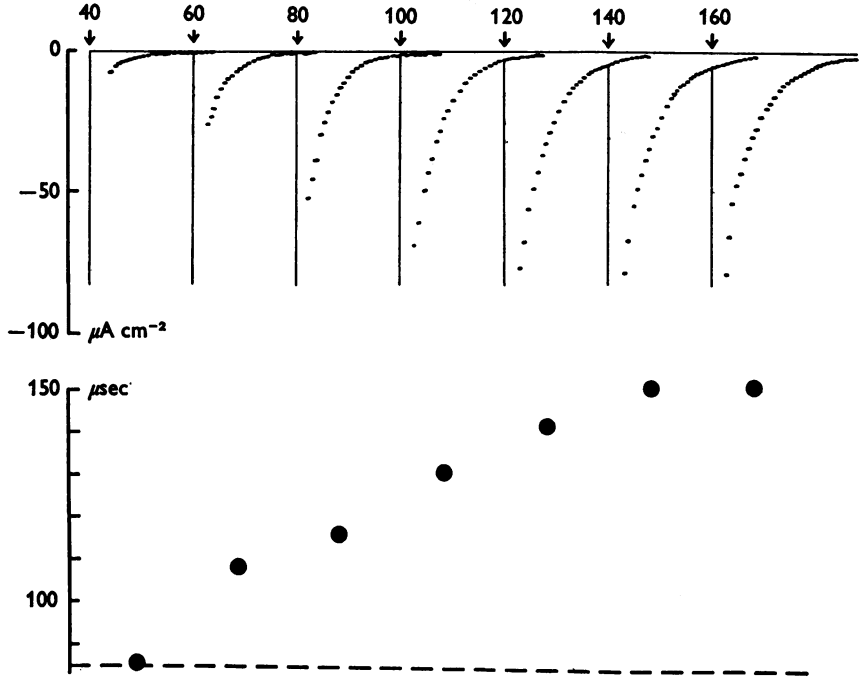

Fig. 15. The effect of pulse size on the time constant of the gating current tail at a constant holding potential. Expt. 20–D–1, fibre internally perfused with high caesium and bathed in tris-SW made with isethionate in place of chloride, $V_h = -100$ mV. Gating current tail transients are shown in the upper part of this figure with the pulse size in mV indicated next to each trace. The corresponding time constants are plotted beneath. Temperature 6·4° C.

one quarter. The results show that in every case $\tau(V)_{off}$ increased progressively as V_p became more positive, the average change for V_p's between about -10 and $+40$ mV being $+34 \pm 8\%$. At the same time, $\tau_{Na,off}$ remained constant within the accuracy of the measurements. The ratio of the two time constants showed a consistent increase both with pulse size and with holding potential, from 1·6 for small pulses applied at a holding potential of -60 mV to $3{\cdot}33 \pm 0{\cdot}15$ for large pulses applied at holding potentials of -90 or -100 mV. In the light of these figures, it is no longer

possible to argue that there is a serious discrepancy between $\tau_{Na,off}$ and $\frac{1}{3}\tau(V)_{off}$, as long as V_p is large and positive and the sodium system is fully primed by making V_h large and negative. Our own earlier conclusion to the contrary (Keynes & Rojas, 1974) was evidently due to inadequate series resistance compensation, the determination of $\tau_{Na,off}$ having been made with full external sodium. It seems possible that Bezanilla & Armstrong (1975) were also using less complete compensation than they

TABLE 4. Comparison of the time constants for turning off the sodium conductance and for the gating current tail during repolarization

Expt. no.	Holding potential V_h (mV)	Pulse potential V_p (mV)	Conductance time constant $\tau_{Na,off}$ (μsec)	Temp. (°C)	Gating current time constant $\tau(V)_{off}$ (μsec)	Temp. (°C)	Ratio
18–D–1	−60	−20	89	7·5	144	7·0	1·62
	−60	0	90	7·5	173	7·0	1·92
	−60	20	91	7·5	187	7·0	2·05
	−60	40	91	7·5	202	7·0	2·22
	−100	−20	47	7·0	94	6·8	2·00
	−100	0	47	7·0	97	6·8	2·06
	−100	20	48	7·0	115	6·8	2·39
	−100	40	50	7·0	151*	6·8	3·02
20–D–1	−60	30	101	6·8	180*	6·4	1·80
	−60	49	102	6·8	202*	6·4	1·98
	−60	57·5	103	6·8	230*	6·4	2·23
	−100	−9	36	6·5	110*	6·4	3·05
	−100	10	36	6·5	122*	6·3	3·39
	−100	27·5	37	6·5	130*	6·3	3·51
	−100	41	38	6·5	131*	6·3	3·45
20–D–3	−90	−12	37·5	7·0	119	7·0	3·17
	−90	1	38	7·0	112	7·0	2·94
	−90	19	37	7·0	125	6·5	3·38
	−90	45	41	7·0	144	6·5	3·51

All fibres were perfused with high $Cs^+ - 1$. $\tau_{Na,off}$ was measured in $\frac{1}{4}$Na-SW. Asterisked values were estimated from single-sweep current records.

supposed, and in any case their measurements were made with $V_h = -70$ mV and $V_p = 0$ to 20 mV, under which conditions we agree that the time constant ratio is less than 2. In addition, the absolute magnitude of their values for the gating current time constant, which apparently had a maximum of about 300 μsec at 2° C, seems surprisingly much smaller than our figure of 460 μsec at 6·3° C (Fig. 13), suggesting that they may have been in error from time-dependent leakage currents of the kind shown in Fig. 14.

If, as has been proposed by Keynes (1975), a further rapid conformational change intervenes between the movements of the gating particles in the electric field and the opening and closing of the sodium channels to the passage of ions, $\tau_{Na,off}$ might be expected to be slightly greater than $\frac{1}{3}\tau(V)_{off}$. The occurrence of such a process with a time constant in the neighbourhood of, say, 20 μsec, cannot be ruled out by any of our comparisons between $\tau(V)$ and τ_m; and if it involved hydrogen bond formation, and hence was appreciably slowed in the presence of deuterium, it would go some way towards explaining Meves's (1974) observations on the action of heavy water. However, Table 4 suggests that for the largest values of V_h and V_p the time constant ratio may actually rise above 3, the genuineness of this trend being supported by the observation of similar behaviour at the node of Ranvier (W. Nonner, E. Rojas and R. Stämpfli, in preparation). There is still much to be learnt from careful comparisons between the sodium conductance and gating current time constants under different experimental conditions.

It remains to provide an explanation for the constancy of $\tau_{Na,off}$ with varying pulse size in contrast to the progressive change in $\tau(V)_{off}$. A plausible hypothesis would be that in any channel where all three of the gating particles have made the voltage-dependent transition to the active configuration, an interaction then takes place between them that both opens the channel and modifies their structure in such a way that their relaxation time for the reverse transition on repolarization of the membrane is about one third greater than it would otherwise be. For small pulses accompanied by opening of relatively few of the channels, a correspondingly small proportion of the particles would display an increased relaxation time during the tail. But for pulses large enough to open all the channels, the relaxation time would be raised for the whole population of particles. Whatever the pulse size or duration, there would be a fixed relationship between $\tau_{Na,off}$ and the value of $\tau(V)_{off}$ for the modified particles. A consequence of this idea that could be tested experimentally would be that the gating current tail for a pulse taking V_p to the midpoint of the m_∞^3 curve should exhibit a 50/50 mixture of the two relaxation times, rather than decaying with a single time constant of intermediate size. However, very good records would be needed to distinguish decisively between the two alternatives.

We are indebted to the Medical Research Council for the appointment of E.R. as a Visiting Senior Scientist under Project Grant G973/437/B, and for the provision of equipment. Mr S. B. Cross gave invaluable assistance with many aspects of the work. Thanks are also due to Dr B. Rudy for help with some of the experiments, and to Dr W. Nonner for providing the computer programs used for least-squares curve fitting.

REFERENCES

ARMSTRONG, C. M. & BEZANILLA, F. (1973). Currents related to movement of the gating particles of the sodium channels. *Nature, Lond.* **242**, 459–461.

ARMSTRONG, C. M. & BEZANILLA, F. (1974). Charge movement associated with the opening and closing of the activation gates of the Na channels. *J. gen. Physiol.* **63**, 533–552.

ARMSTRONG, C. M., BEZANILLA, F. & ROJAS, E. (1973). Destruction of sodium conductance inactivation in squid axon perfused with pronase. *J. gen. Physiol.* **62**, 375–391.

BEZANILLA, F. & ARMSTRONG, C. M. (1975). Kinetic properties and inactivation of the gating currents of sodium channels in squid axon. *Phil. Trans. R. Soc.* B **270**, 449–458.

BEZANILLA, F., ROJAS, E. & TAYLOR, R. E. (1970). Sodium and potassium conductance changes during a membrane action potential. *J. Physiol.* **211**, 729–751.

COHEN, L. B., HILLE, B., KEYNES, R. D., LANDOWNE, D. & ROJAS, E. (1971). Analysis of the potential-dependent changes in optical retardation in the squid giant axon. *J. Physiol.* **218**, 205–237.

CONTI, F., DE FELICE, I. J. & WANKE, E. (1975). Potassium and sodium ion current noise in the membrane of the squid giant axon. *J. Physiol.* **248**, 45–82.

DODGE, F. A. & FRANKENHAEUSER, B. (1959). Sodium currents in the myelinated nerve fibre of *Xenopus laevis* investigated with the voltage clamp technique. *J. Physiol.* **148**, 188–200.

FRANKENHAEUSER, B. (1960). Quantitative description of sodium currents in myelinated nerve fibres of *Xenopus laevis*. *J. Physiol.* **151**, 491–501.

FRANKENHAEUSER, B. & HODGKIN, A. L. (1956). The after-effects of impulses in the giant nerve fibres of *Loligo*. *J. Physiol.* **131**, 341–376.

GLASSTONE, S., LAIDLER, K. J. & EYRING, H. (1941). *The Theory of Rate Processes.* New York-London: McGraw Hill.

HODGKIN, A. L. & HUXLEY, A. F. (1952*a*). The components of membrane conductance in the giant axon of *Loligo*. *J. Physiol.* **116**, 473–496.

HODGKIN, A. L. & HUXLEY, A. F. (1952*b*). A quantitative description of membrane current and its application to conduction and excitation in nerve. *J. Physiol.* **117**, 500–554.

KETTERER, B., NEUMCKE, B. & LÄUGER, P. (1971). Transport mechanism of hydrophobic ions through lipid bilayer membranes. *J. membrane Biol.* **5**, 225–245.

KEYNES, R. D. (1975). Organization of the ionic channels in nerve membranes. In *The Nervous System*, vol. 1, *The Basic Neurosciences*, ed. TOWER, D. B. New York: Raven Press.

KEYNES, R. D., BEZANILLA, F., ROJAS, E. & TAYLOR, R. E. (1975). The rate of action of tetrodotoxin on sodium conductance in the squid giant axon. *Phil. Trans. R. Soc.* B **270**, 365–375.

KEYNES, R. D. & ROJAS, E. (1974). Kinetics and steady-state properties of the charged system controlling sodium conductance in the squid giant axon. *J. Physiol.* **239**, 393–434.

KEYNES, R. D., ROJAS, E. & RUDY, B. (1974). Demonstration of a first-order voltage-dependent transition of the sodium activation gates. *J. Physiol.* **239**, 100–101*P*.

KEYNES, R. D., ROJAS, E., TAYLOR, R. E. & VERGARA, J. (1973). Calcium and potassium systems of a giant barnacle muscle fibre under membrane potential control. *J. Physiol.* **229**, 409–455.

LEVINSON, S. R. & MEVES, H. (1975). The binding of tritiated tetrodotoxin to squid giant axons. *Phil. Trans. R. Soc.* B **270**, 349–352.

MEVES, H. (1974). The effect of holding potential on the asymmetry currents in squid giant axons. *J. Physiol.* **243**, 847–867.

MOORE, J. W. & COLE, K. S. (1962). Voltage clamp techniques. In *Physical Techniques in Biological Research*, ed. NASTUK, W. L. New York: Academic Press.

NONNER, W., ROJAS, E. & STÄMPFLI, R. (1975). Displacement currents in the node of Ranvier. Voltage and time dependence. *Pflügers Arch. ges. Physiol.* **354**, 1–18.

ROJAS, E. & KEYNES, R. D. (1975). On the relation between displacement currents and activation of the sodium conductance in the squid giant axon. *Phil. Trans. R. Soc.* B **270**, 459–482.

ROJAS, E., TAYLOR, R. E., ATWATER, I. & BEZANILLA, F. (1969). Analysis of the effects of calcium or magnesium on voltage-clamp currents in perfused squid axons bathed in solutions of high potassium. *J. gen. Physiol.* **54**, 532–552.